12th Int. Particle Acc. Conf. IPAC2021, Campinas, SP, Brazil JACoW Publishing
ISBN: 978-3-95450-214-1 ISSN: 2673-5490 doi:10.18429/JACoW-IPAC2021-WEPAB008

NUMERICAL NOISE STUDY IN EIC BEAM-BEAM SIMULATIONS*

D. Xu†, Y. Luo, C. Montag, Brookhaven National Laboratory, Upton, NY, USA
Y. Hao, Michigan State University, East Lansing, MI, USA
J. Qiang, Lawrence Berkeley National Laboratory, Berkeley, CA, USA

Abstract

In the Electron-Ion Collider (EIC) design, a flat beam collision scheme is adopted to achieve 10^{34} cm^{-2}s^{-1} luminosity. We found that the vertical growth of the proton beam is much larger than of the round beam. In this article we present the numerical noise study about the number of macroparticles, the electron slice number, and the electron bunch length. Both weak-strong and strong-strong simulation methods are used. It turns out the proton emittance growth in the strong-strong simulation mainly comes from the numerical noise. This study helps us to perform beam-beam simulation correctly for the EIC.

INTRODUCTION

Compared with the electron beam, the radiation for ions in the EIC is negligible. The cooling time of the ion beam is expected to be 1 hour due to strong hadron beam cooling [1], which is much longer than typical radiation damping time. As a result, the ion beam lifetime determined by beam-beam interaction in the EIC is an important issue.

In the EIC, the ion beam will collide with the electron beam with a total crossing angle of 25 mrad. In [2], we demonstrated that the dominant physical reason affecting the ion beam emittance growth is the synchro-betatron resonance, which is caused by the nonlinear crab kick from the crab cavity. Two feasible methods can be used to mitigate the emittance growth without sacrificing the luminosity — the tune optimization [3] and the combination of harmonic crab cavities [4].

In this paper, the parameters are taken from the EIC Conceptual Design Report (CDR). The optimization procedure is described in [5]. The simulation studies use the strong-strong code BeamBeam3D [6] and a self-written weak-strong code.

PROBLEM

Table 1 lists the beam parameters as presented in the EIC CDR. Figure 1 shows the corresponding simulation results by strong-strong tracking. The electron beam distribution reaches equilibrium in about 20,000 turns (4 damping times), and the remaining 30,000 turns are used to determine the proton beam growth rate. In Fig. 1, both curves overlap with each other. It means that the emittance growth driven by the synchro-betatron resonances in the crab crossing scheme is comparable with the head-on situation. However, the growth rates in the horizontal or vertical plane are 1000%/h and 2500%/h. Those numbers would be unacceptable in a real machine.

Table 1: Flat Beam Parameters in the EIC CDR

Quantity	Unit	Proton	Electron
Crossing angle	mrad	25	
Beam energy	GeV	275	10
Bunch intensity	10^{11}	0.668	1.72
β^* at IP	cm	80/7.2	55/5.6
Beam sizes at IP	µm	95/8.5	
Bunch length	cm	6	2
Transverse tunes		0.228/0.210	0.08/0.06
Longitudinal tune		0.01	0.069

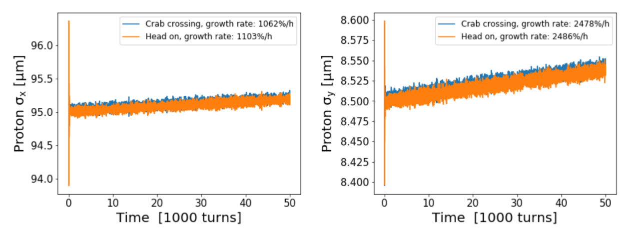

Figure 1: Beam size evolution for the EIC CDR by strong-strong tracking.

It is well-known that the Particle-in-cell (PIC) algorithm is subject to numerical noise [7]. In Beambeam3D, a computational grid is used to calculate the beam-beam force from an arbitrary beam distribution. It deposits the macroparticles on the grid and then solves the Poisson equation. A round beam simulation is performed with the same grid size to get a sense of how the numerical noise affects the growth number. In this simulation, parameters of two beams are same except for the sign of the charge number. Table 2 lists the beam parameters taken from RHIC e-lens project [8]. Table 3 shows the code setup in the two simulations. Figure 2 compares the two simulation results. The beam-beam parameters in Table 1 and Table 2 are similar. However, the growth rate in the round beam simulation is much smaller than the flat beam.

It is necessary to understand the difference. In the flat beam scheme, the vertical emittance is ten times smaller than the horizontal one. Physically, the higher-order betatron and synchro-betatron resonances are unavoidable. Even a weak coupling may cause the vertical emittance growth. Numerically, vertical emittance is more vulnerable to numerical noise. We need to find out which one is dominant.

* Work supported by Brookhaven Science Associates, LLC under Contract No. DE-SC0012704 with the U.S. Department of Energy
† dxu@bnl.gov

ISBN: 978-3-95450-214-1 ISSN: 2673-5490 doi:10.18429/JACoW-IPAC2021-WEPAB008

Table 2: Beam Parameters for Round Beam Simulation

Quantity	**Unit**	**Proton**	**Anti-Proton**
Crossing angle	mrad	0	
Beam energy	GeV	250	250
Bunch intensity	10^{11}	2	2
β^* at IP	cm	50/50	50/50
Beam sizes at IP	µm	70/70	
Bunch length	cm	25	25
Transverse tunes		0.228/0.210	
Longitudinal tune		0.01	0.01

Table 3: Code Setup in the Flat and Round Beam Simulation

Type	**Flat**	**Round**
Grid size	128 × 128	
Macro partilcles [10^6]	1.0/1.0	0.5/2.0
Longitudinal slices	45/45	7/21

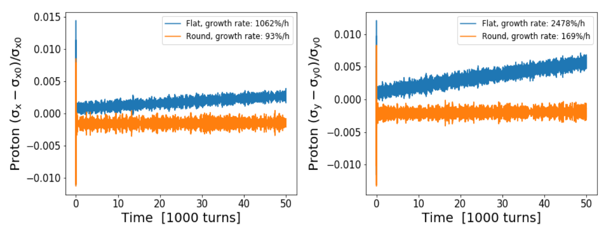

Figure 2: The comparison of strong-strong simulation between the flat and the round beam collision.

WEAK-STRONG STUDY

Weak-strong simulation is a convenient tool to study the dynamics of a single particle. If there exist strong resonances, a degradation will be present in the weak-strong simulation. In our study, the electron beam is a rigid Gaussian beam. The beam parameters are listed in Table 1.

The first factor that affects the growth rate is the slice number of the electron beam. Figure 3 shows the simulation results. The number of macroparticles is 2 million. The proton beam is tracked over 100,000 turns. The horizontal growth rate is always negligible. The vertical growth rate saturates with more than 6 slices. There is no significant improvement when further increasing the slice number.

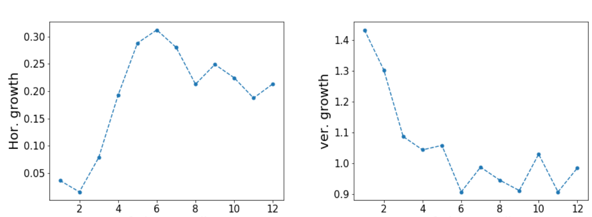

Figure 3: Beam size evolution for different number of electron slices by weak-strong tracking.

The second factor is the number of macroparticles. As more macroparticles are used, there is less Monte Carlo noise. The simulation results are present in Fig. 4. The oscillation amplitude of σ_x or σ_y becomes smaller. However, the vertical growth rate doesn't scale down. It seems that one or two million macroparticles are sufficient in weak-strong simulation.

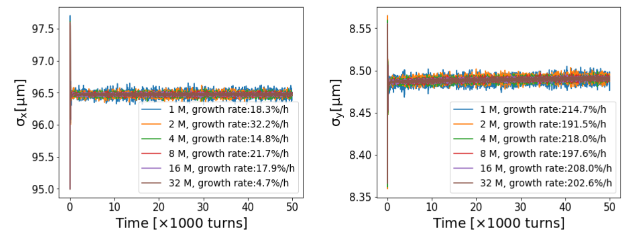

Figure 4: Beam size evolution for different number of macro particles. The word "million" is abbreviated as M in the legend.

The fitting length and the tracking time may affect the growth rate too. The effect can be both numerical and physical. On the one hand, the beam sizes change turn by turn due to the betatron oscillation and the Monte Carlo noise; on the other hand, the beam-beam force gets weaker as the proton particles diffuse. Figure 5 shows the simulation result with a much longer tracking time. The growth rate is then largely reduced. The electron beam is represented by the one slice model. Figure 6 shows the growth rate at different times. The fitting length is 50 thousand turns. From Fig. 6, a half-million turns are needed in the weak-strong simulation.

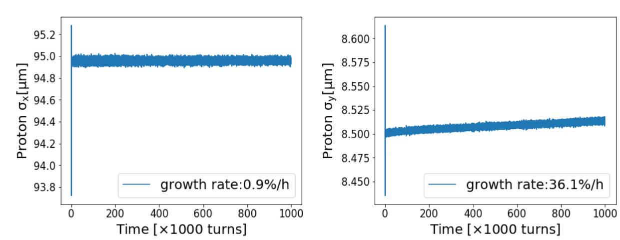

Figure 5: Beam size evolution for 1 million turns by weak-strong tracking.

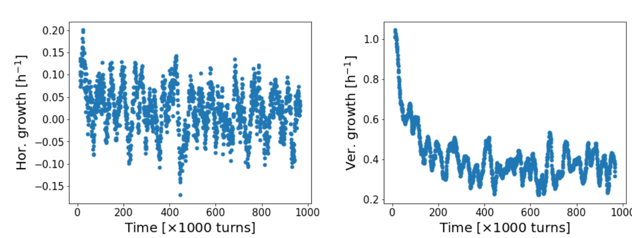

Figure 6: Growth rates at different times. The fitting length is 50 thousand turns.

ISBN: 978-3-95450-214-1 ISSN: 2673-5490 doi:10.18429/JACoW-IPAC2021-WEPAB008

STRONG-STRONG STUDY

However, the strong-strong simulation can't be tracked as long as a half-million turns due to the limitation of computation resources. In our study, we track particles over 50,000 turns and then compare the growth rates for different parameters. The transverse working points for the electron and proton beam are $(0.070, 0.139)$ and $(0.355, 0.193)$ based on our tune scan results [3]. Other parameters are the same as Table 1 after electron beam reaches its equilibrium. The high-order harmonic crab cavity is also used in the proton ring as suggested by [4].

Firstly, the number of electron macroparticles N^e is scanned. Figure 7 shows the simulation results. There is little benefit when $N^e > 3$ M. Then the electron slice number n_s^e and the number of electron macroparticles are scanned together. The simulation results are present in Fig. 8. When $N^e = 2$ M and $n_s^e = 28$, the growth rates have the same magnitude as for the round beams in Fig. 2. It turns out that the difference between the round and the flat beam collision mostly comes from the numerical noise. The longitudinal smoothing can not be neglected in the strong-strong simulation.

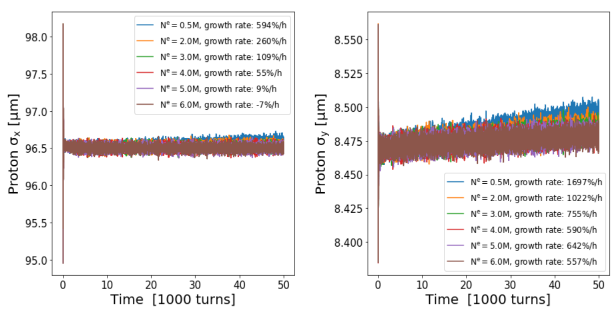

Figure 7: Beam size evolution in strong-strong simulation when scaling the electron macroparticles.

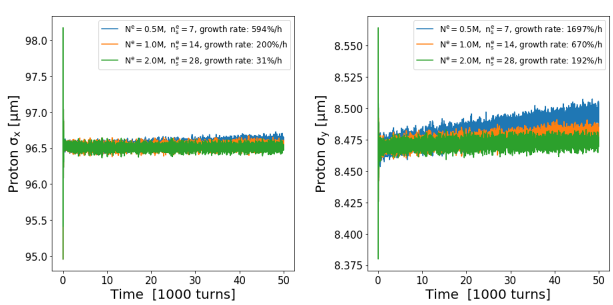

Figure 8: Beam size evolution in strong-strong simulation when scaling the electron slices and macroparticles.

Different from the weak-strong simulation, the slice number seems more important in the strong-strong simulation. To further comfirm that, dependence of the effect of the number of slices for different bunch lengths is studied. The simulation results are shown in Fig. 9. In principle, the shorter electron beam will make the proton beam lifetime worse. But there is no such dependence in Fig. 9. The major difference is from the slice number. The results suggest that we cannot reduce the slice number even if the electron beam is very short.

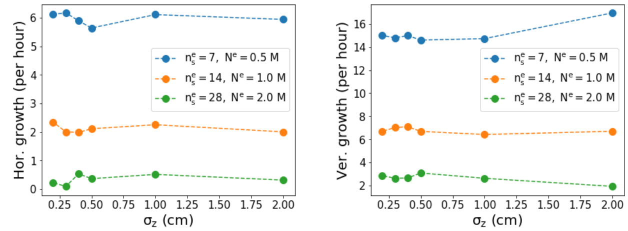

Figure 9: Dependence of the effect of the number of slices for different electron bunch length.

SUMMARY

In this article, we present the numerical noise study by weak-strong and strong-strong model for the EIC beam-beam simulation. In weak-strong simulation, a half-million turns are necessary to determine the growth rate. In strong-strong simulation, the growth rate mainly stems from the numerical noise. By scaling the electron slice number and the number of electron macroparticles, the proton growth rate is reduced to the same level of the round beam collision. Our simulation also shows that the electron slice number cannot be reduced even if the electron beam is very short. The quantitative understanding of the numerical noise is still ongoing.

REFERENCES

[1] G. Stupakov and P. Baxevanis, "Microbunched electroncooling with amplification cascades", *Phys. Rev. Accel.Beams*, vol. 22, p. 034401, 2019. doi:10.1103/PhysRevAccelBeams.22.034401

[2] D. Xu *et al.*, "Synchrobeta-tron resonance of crab crossing scheme with large crossingangle and finite bunch length", *Phys. Rev. Accel. Beams*, vol. 24, p. 041002, 2021. doi:10.1103/PhysRevAccelBeams.24.041002

[3] D. Xu, Y. Hao, Y. Luo, C. Montag, and J. Qiang, "Full Range Tune Scan Studies Using Graphics Processing Units With CUDA in EIC beam-beam Simulations", presented at the 12th Int. Particle Accelerator Conf. (IPAC'21), Campinas, Brazil, May 2021, paper WEPAB010.

[4] D. Xu, Y. Hao, Y. Luo, C. Montag, and J. Qiang, "Study of Harmonic Crab Cavity in EIC Beam-Beam Simulations", presented at the 12th Int. Particle Accelerator Conf. (IPAC'21), Campinas, Brazil, May 2021, paper WEPAB009.

[5] Y. Luo *et al.*, "Beam-Beam Related Design Parameter Optimization for the Electron-Ion Collider", presented at the 12th Int. Particle Accelerator Conf. (IPAC'21), Campinas, Brazil, May 2021, paper THPAB028.

[6] J. Qiang *et al.*, "A Parallel Particle-In-Cell Model for Beam-Beam Interactions in High Energy Ring Colliders", *J. Comp. Phys.*, vol. 198, pp. 278–294, 2004. doi:10.1016/j.jcp.2004.01.008

[7] F. Kesting and G. Franchetti, "Propagation of numerical noise in particle-in-cell tracking", *Phys. Rev. Accel.Beams*, vol. 18, p. 114201, 2015. doi:10.1103/PhysRevSTAB.18.114201

[8] W. Fischer *et al.*, "Status of the RHIC head-on beam-beam compensation project", Brookhaven National Laboratory, United States, Rep. BNL-94072-2011-CP, Jan. 2010.